Performance Analysis of IEEE 802.15.4 Beacon-Enabled Mode

Chiara Buratti, *Member, IEEE*

***Abstract*—In this paper, a mathematical model for the beacon-enabled mode of the IEEE 802.15.4 medium-access control (MAC) protocol is provided. A personal area network (PAN) composed of multiple nodes, which transmit data to a PAN coordinator through direct links or multiple hops, is considered. The application is query based: Upon reception of the beacon transmitted by the PAN coordinator, each node tries to transmit its packet using the superframe structure defined by the IEEE 802.15.4 protocol. Those nodes that do not succeed in accessing the channel discard the packet; at the next superframe, a new packet is generated. The aim of the paper is to develop a flexible mathematical tool able to study beacon-enabled 802.15.4 networks organized in different topologies. Both the contention access period (CAP) and the contention-free period defined by the standard are considered. The slotted carrier-sense multiple access with collision avoidance (CSMA/CA) algorithm used in the CAP portion of the superframe is analytically modeled. The model describes the probability of packet successful reception and access delay statistics. Moreover, both star and tree-based topologies are dealt with; a suitable comparison between these topologies is provided. The model is a useful tool for the design of MAC parameters and to select the better topology. The mathematical model is validated through simulation results. The model differs from those previously published by other authors in the literature as it precisely follows the MAC procedure defined by the standard in the context of the application scenario described.**

***Index Terms*—Carrier-sense multiple access with collision avoidance (CSMA/CA), guaranteed time slots (GTSs), IEEE 802.15.4, medium-access control (MAC), tree-based topology, Zigbee.**

I. Introduction

IEEE 802.15.4 [1], [2] is a short-range wireless technology intended to provide applications with relaxed throughput and latency requirements in wireless personal area networks (PANs). The key features of 802.15.4 are low complexity, low cost, low power consumption, and low data rate transmissions.

In this paper, we consider a PAN composed of multiple devices (hereafter denoted as nodes) that have to transmit data to the PAN coordinator through single or multiple hops. We assume that the application requires periodic data at the PAN coordinator: Each node, upon reception of a query coming from the PAN coordinator, generates a packet and attempts to access the channel to transmit it. Therefore, each node has only one packet per query to be transmitted. If the node does not succeed in accessing the channel before the reception of the next query, the packet is lost, and a new one is generated.

Examples of application of this scenario to realistic cases can easily be found, e.g., in the context of body area networks [3], [4] or wireless sensor networks (WSNs) [5]–[7]. IEEE 802.15.4, in fact, is one of the most suitable technologies for WSNs. In most WSN applications, nodes are distributed over an environment with the aim of estimating a spatial process [5], like temperature or pressure: Nodes periodically take samples of the process from the environment to transmit it toward a data collector (i.e., the PAN coordinator in our scenario).

Both star and tree-based topologies are accounted for. In particular, first, we deal with a star topology that could be used when the number of nodes in the network is small (however, for the sake of validation of the model, results for larger networks are also shown). Then, a tree rooted at the PAN coordinator is studied.

No connectivity issues are considered in this paper; in the star topology case, it is assumed that all nodes can reach the coordinator, whereas in the tree-based topology case, we assume that the children of a given parent may reach the parent itself.

The 802.15.4 standard allows the following two types of channel access mechanisms: 1) beacon enabled (this option is mandatory when tree topologies are used) and 2) non-beacon enabled. The latter case uses unslotted carrier-sense multiple access with collision avoidance (CSMA/CA), whereas in the former, a slotted CSMA/CA algorithm and a superframe structure managed by the PAN coordinator is used. As will be described in the following, the superframe starts with a packet transmitted by the PAN coordinator, which is denoted as beacon, and could include some slots allocated to given nodes, called guaranteed time slots (GTSs).

Since periodic data acquisition at the PAN coordinator is required, the beacon-enabled mode is used; therefore, the beacon packet will coincide with the query.

Given the scenario described above, the scope of this paper is to provide a mathematical model for the description of the probability of packet successful reception and access delay statistics.

To such aim, the transitions between node states (backoff, sensing, transmit, idle) of the slotted CSMA/CA 802.15.4 medium-access control (MAC) protocol have to be modeled. The probabilities of channel access and successful transmission are evaluated as a function of time, starting from reception of the beacon sent by the coordinator until the end of the superframe. The model also allows the evaluation of the

Manuscript received May 4, 2009; revised October 29, 2009 and December 1, 2009. First published January 12, 2010; current version published May 14, 2010. This work was supported by the European Commission in the framework of the FP7 Network of Excellence in Wireless COMmunications NEWCOM++ under Contract 216715. The review of this paper was coordinated by Dr. J. Deng.

The author is with the Wireless Communications LABoratory in Bologna, Department of Electronics, Computer Science, and Robotics, University of Bologna, 40136 Bologna, Italy (e-mail: c.buratti@unibo.it).

Color versions of one or more of the figures in this paper are available online at http://ieeexplore.ieee.org.

Digital Object Identifier 10.1109/TVT.2010.2040198

overall success probability for a packet to be transmitted—the throughput—i.e., the number of bytes per unit of time successfully received by the coordinator and the average delays. Performance is evaluated by changing the number of nodes, the duration of the superframe, the number of GTSs, and the packet size. To validate the mathematical model, comparison to simulations is performed, and results show an almost perfect match. Performance metrics are first evaluated for the star topology case, and then, the model is applied to a three-level tree-based topology, and a suitable comparison between the two topologies is shown. Extension to the case of tree of any height is trivial.

This paper is outlined as follows. An overview of the literature is provided in Section II, Section III describes the IEEE 802.15.4 MAC protocol, Section IV deals with the scenario and the model assumptions, Section V introduces the metrics derived from the model, and in Sections VI and VII, the mathematical model of the slotted CSMA/CA algorithm and the related performance metrics are derived. Sections V–VII are related to the star topology. The tree-based topology is discussed in Section VIII, and numerical results for both the topologies are shown in Section IX. Finally, conclusions are reported in Section X. Part of the analytical formulation is left to the Appendix.

II. Related Works

In the literature, there exist several works devoted to the study of 802.15.4 networks. Performance evaluation of the 802.15.4 MAC protocol has been carried out by means of simulations [8]–[10]. Additionally, some studies have tried to analytically describe the behavior of the 802.15.4 MAC protocol, as this paper does. However, none of them captures the exact essence of the IEEE 802.15.4 MAC in the scenario described here.

The model described in [11] fails to match simulation results, as described in [12], as the authors use the same Markov formulation and assumptions made by Bianchi [13], where the 802.11 MAC protocol is considered. This protocol, in fact, is significantly different from the one defined by the 802.15.4 standard [14]. A better model is proposed in [15], where the probabilities of being in sensing in the two subsequent slots are not correctly captured by the Markov chain (see also [12]). In [16], the events of finding the channel free in the first and second slots are considered independent, and the probabilities that those two events happen are assumed to be equal. As will be clarified in the following, instead, these events are not independent, and this approximation causes notable differences between simulations and analytical results. Another model is presented in [17], where different simplifying assumptions are made: The uniform distribution of the backoff counter within the backoff windows is assumed to be geometrically distributed so that the backoff algorithm becomes memoryless. The model developed in [17] has been validated through simulations but only for a very small set of parameters, and only a network composed of 12 nodes is considered.

However, all the above cited works (also [12] and [17], which seem to provide the better models) are based on Bianchi's model and use a Markov chain to describe node states, even if the process representing the backoff time counter is not Markovian since the value of the backoff counter depends on the past history (i.e., how many times the node has tried to access the channel and found it busy). To use a Markov chain, in fact, Bianchi assumes that at each transmission attempt, and regardless of the number of retransmissions suffered (backoff stages in the 802.15.4 case), each packet collides with constant and independent probability (see [13]). This assumption results more accurate as long as the contention window and the number of nodes accessing the channel get larger. This approximation is good for the aforementioned works, being the number of nodes competing for the channel constant in time; however, it is not accurate for query-based applications. In the scenario considered here, in fact, the number of nodes accessing the channel decreases by passing time (since nodes have only one packet to be transmitted per superframe upon reception of the query), resulting in a decreasing of the probability that a packet collides. The difference of the scenarios studied here and in the previous works, in fact, completely changes the form of the analysis. In the previous works, it is assumed that nodes always [12], [13], [15], or with a certain probability [11], [18]–[20], have a packet to be transmitted (in [17], Poisson distributed arrivals of packets is assumed). This means that once a node transmits its packet, it will start the backoff algorithm again, possibly with a certain probability, which is known. In our model, on the contrary, the number of nodes competing for channel access decreases with time. Therefore, according to the different scenario studied, the aforementioned assumption is removed here, and the probabilities (of being in sensing and transmission and of colliding) are evaluated for the different backoff stages and the different instants of time.

Moreover, one of the most important aims of this paper is to derive the access delay statistics. Since all the works cited [11]–[13], [15]–[17] studied the asymptotic behavior of the network at the equilibrium conditions, evaluating the stationary probabilities obtained when time tends to infinite, the statistics of traffic cannot be derived from these analyses.

Finally, it is worth noting that the works present in the literature do not analytically account for the modeling of GTSs, the duration of the superframe (which strongly affects performance, as shown in this paper), and tree-based topologies. All these issues, instead, are considered in this paper.

This paper is based on previous works [14], [21], where the non beacon-enabled mode is analyzed. Even though the rationale used to derive the metrics is similar, the presence of the two subsequent sensing phases, characterizing the slotted CSMA/CA of the beacon-enabled mode, significantly changes the model with respect to [14] and [21]: A different finite-state-transmission diagram for modeling nodes states is needed, and the formulas for deriving the sensing and transmission probabilities are different. Moreover, in the beacon-enabled mode, the events of being in sensing in the two different phases and to find the channel free are not independent (as will be clear in the following, a node enters in the second sensing phase only when it finds the channel free in the first phase). This dependence makes the model developed here very different and more complex than the one developed in [14] and [21]. Finally,

here, tree-based topologies are studied, whereas in [14] and [21], only star topologies are considered since the non beacon-enabled mode does not allow the formation of trees.

III. IEEE 802.15.4 Medium-Access Control Protocol

According to the IEEE 802.15.4 MAC protocol in beacon-enabled mode [1], the access to the channel is managed through a superframe, starting with the beacon packet transmitted by the PAN coordinator. The superframe is subdivided into the following three parts: 1) an inactive part; 2) a contention access period (CAP), during which nodes use a slotted CSMA/CA; and 3) a contention-free period (CFP), containing a number of GTSs that can be allocated by the PAN coordinator to specific nodes. The PAN coordinator may allocate up to seven GTSs, but a sufficient portion of the CAP must remain for contention-based access. The minimum CAP duration is equal to 440 T_s, where T_s is the symbol time. Here, we consider the 2.45 GHz band, meaning a symbol rate of 62.5 ksymbols/s, which brings to have $T_s = 16$ μs [1].

The duration of the active part and of the whole superframe depends on the value of the following two integer parameters both ranging from 0 to 14: 1) the superframe order, denoted as SO, and 2) the beacon order, denoted as BO, where $BO > SO$. The latter defines the interval of time between two successive beacons, namely, the beacon interval, denoted as T_B, which is given by $T_B = 960 \cdot 2^{BO} \cdot T_s$. The duration of the active part of the superframe, containing CAP and CFP, namely, the superframe duration, denoted as T_A, is given by $T_A = 960 \cdot 2^{SO} \cdot T_s$.

The inactive part (present when $BO > SO$) is used for saving energy (nodes can switch off during this phase) or for exploiting multihops. Since the evaluation of energy consumption is out of scope of this paper, we set $SO = BO$ (i.e., $T_B = T_A$) in case of star topologies (one hop) and $BO > SO$ for trees. A proper setting of the parameters BO and SO in the latter case is needed: Section IX-B tries to provide some guidelines for this setting.

The CSMA/CA algorithm used in the CAP portion of the superframe is implemented using units of time called backoff periods: A backoff period has a duration, denoted as $d_{\rm bo}$, equal to 20 $T_s = 320$ μs. The backoff period boundaries of every node in the PAN must be aligned with the superframe slot boundaries of the coordinator; therefore, the beginning of the first backoff period of each node is aligned with the beginning of the beacon transmission. Moreover, all transmissions may start on the boundary of a backoff period.

Each node maintains the following three variables for each transmission attempt: 1) NB; 2) CW; and 3) BE. NB is the number of times the CSMA/CA algorithm was required to backoff while attempting the current transmission. CW is the number of backoff periods that need to be clear of channel activity before the transmission can start. BE is the backoff exponent related to the maximum number of backoff periods that a node will wait before attempting to assess the channel.

The algorithm follows the following steps (see Fig. 1). First, NB, CW, and BE are initialized to 0, 2, and $BE_{\min}$, respectively. Upon reception of the beacon, any activity is delayed

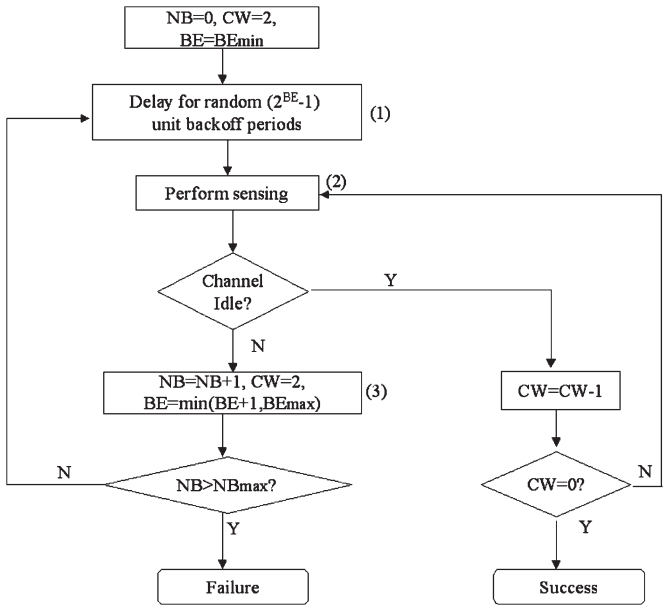

Fig. 1. IEEE 802.15.4 CSMA/CA algorithm.

(backoff state) for a random number of backoff periods in the range (0, $2^{BE} - 1$) [step 1)]. After this delay, channel sensing is performed for one backoff period [step 2)]. If the channel is assessed to be busy, CW is set to 2, and NB and BE are increased by 1, ensuring that BE is not larger than $BE_{\max}$. If the value of NB is lower than $NB_{\max}$, the algorithm returns to step 1); otherwise, the algorithm will unsuccessfully terminate, which means that the node does not succeed in accessing the channel. If the channel is assessed to be idle, instead, CW is decremented by 1 and compared with 0. If $CW > 0$, the algorithm returns to step 2); otherwise, a transmission may start.

IV. Reference Scenario and Model Assumptions

We consider a PAN composed of N nodes transmitting packets that are of size z equal to $D \cdot 10$ bytes, with D being an integer in the range [2, 13] according to the minimum and maximum possible data packet size [1]. By assuming a 16-bit short address is used, the data frame has a size of $(6 + 11 + n)$ bytes, where n is the size of the payload in bytes, and 6 and 11 bytes are the physical and MAC overheads [1]. Therefore, in the case $D = 2$, we will have $n = 4$ bytes, and with the maximum packet size equal to 133 bytes, the maximum value of D is 13. The time needed to transmit a packet will be equal to $D \cdot d_{\rm bo}$ as a bit rate of 250 kbits/s is used; therefore, each packet occupies D backoff periods.

We also denote as $N_{\rm GTS}$ the number of GTSs allocated (see Fig. 2 above part). Therefore, in each superframe, $N_{\rm GTS}$ nodes will have a GTS allocated and will use the CFP to transmit their packets, and the remaining $N - N_{\rm GTS}$ nodes will use the CAP portion.

According to the standard, each GTS must have a duration multiple of $60 \cdot 2^{SO} \cdot T_s$; we denote this duration as $d_{\rm GTS}$, which is equal to $D_{\rm GTS} \cdot 60 \cdot 2^{SO} \cdot T_s$, with $D_{\rm GTS}$ integer (see the top part of Fig. 2). Since an interframe space between two successive packets received by the coordinator must be

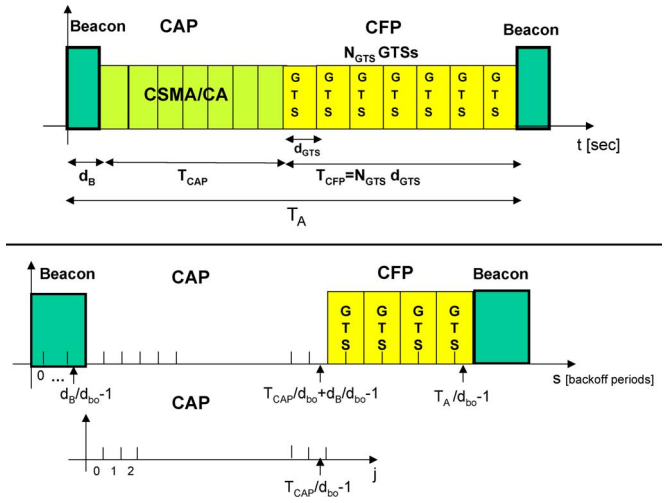

Fig. 2. IEEE 802.15.4 superframe, considering (top) the time axis and (bottom) the number of slots s.

guaranteed, D_{GTS} is derived such that the GTS contains the packet and the interframe space. The interframe space duration depends on the size of the MAC protocol data unit (MPDU): For an MPDU lower than 18 bytes, an interframe space of $12\,T_s$ must be present, whereas $40\,T_s$ is needed for an MPDU larger than 18 bytes [1]. We set the GTS duration equal to the minimum possible duration that allows to contain the packet and the interframe space. Therefore, by denoting as d_{ifs} the duration of the interframe space, we have $D_{\mathrm{GTS}} = \lceil (D \cdot d_{\mathrm{bo}} + d_{\mathrm{ifs}})/(60 \cdot 2^{SO} T_s) \rceil$, and the number of backoff periods occupied by each GTS is equal to $D_{\mathrm{GTS}} \cdot 3 \cdot 2^{SO}$.

Finally, we denote the beacon size as z_B and as d_B the instant in which the CAP starts (see Fig. 2). Since alignment between the first backoff period of each node and the beginning of the beacon transmission is required, d_B will be equal to the beacon transmission time only in the case when it is a multiple of d_{bo}; otherwise, it will be larger.

No hidden terminal problem is accounted for: All nodes competing for the channel can "hear" each other [11]–[13], [15]. The number of nodes competing for the channel that must be audible one to each other is the number of nodes in the network in the star topology case and the children of a given parent in the tree case (see Section VIII). In these conditions, collisions may occur only in case two or more nodes perform sensing at the same time, find the channel free, and transmit simultaneously their packets. For the sake of energy efficiency, no acknowledge and retransmission mechanism is implemented.

Having fixed the origin of time axis at the beginning of the superframe $(t = 0)$ and all nodes will start the CSMA/CA algorithm at $t = d_B$ since no propagation delay is assumed due to short distances. As stated in Section I, we assume that in case a node does not succeed in accessing the channel by the end of the superframe, the packet is lost. According to our application scenario, in fact, it is reasonable to assume that once a node receives a new query, it takes a new sample from the environment instead of trying to transmit the old one.

In the model, the resolution time (hereafter denoted as slot) is set equal to the backoff period d_{bo}, which also corresponds to the duration of the single sensing phase and to the packet transmission time in the (ideal) case $D = 1$.

Therefore, since one of the aims of the model is to derive the statistics of the traffic generated by nodes in the whole superframe, we will study the behavior of the network in each slot. In the following, we will denote as s the sth slot in the superframe, with $s \in [0, T_A/d_{\mathrm{bo}} - 1]$.

V. Performance Metrics Derived From the Model

The model provides the following metrics:

1) the probability that a node ends the transmission of its packet in a given slot s, denoted as $P\{T^s\}$, with $s \in [0, T_A/d_{\mathrm{bo}} - 1]$;
2) the probability that the coordinator receives the packet tail, coming from a node in a given slot s, denoted as $P\{Z^s\}$, with $s \in [0, T_A/d_{\mathrm{bo}} - 1]$;
3) the success probability for a transmission, i.e., the probability that a node succeeds in transmitting its packet in the superframe whatever the slot is, denoted as p_s;
4) the average delay D_{mean}, with which a packet is received by the coordinator.

We assume that when N_{GTS} GTSs are allocated, the coordinator randomly selects the N_{GTS} nodes to which they should be allocated. Therefore, no resource allocation strategies are accounted for. For the scenario considered, this assumption is reasonable since all nodes transmit packets of the same size and no priority policy between nodes is needed. Since each node has only a packet per superframe to be transmitted, it will use the CAP or the CFP (but not both). In these conditions, the probability that a node has a specific GTS allocated is $1/N$, whereas the probability that a node has whatever a GTS allocated (i.e., the probability that the node may use the CFP) is equal to N_{GTS}/N. However, note that the model could be applied to any GTS allocation strategy by simply changing the probability $1/N$.

To simplify the formulas in the following, we will indicate with the integer j the slots in the CAP portion and with $P\{T^j\}_{\mathrm{CAP}}$ and $P\{Z^j\}_{\mathrm{CAP}}$ the probabilities that a node succeeds in accessing the channel and in transmitting its packet in slot j of the CAP portion, with $j \in [0, T_{\mathrm{CAP}}/d_{\mathrm{bo}} - 1]$, where T_{CAP} is the duration of the CAP portion given by $T_{\mathrm{CAP}} = T_A - d_B - N_{\mathrm{GTS}} \cdot d_{\mathrm{GTS}}$. Therefore, we simply set $j = s - d_B/d_{\mathrm{bo}}$ (see Fig. 2).

The probabilities $P\{T^s\}$ and $P\{Z^s\}$ in the CAP portion are given by

$$P\{T^s\} = P\{T^j\}_{\mathrm{CAP}} \cdot \frac{N - N_{\mathrm{GTS}}}{N} \tag{1}$$

for $s \in [d_B/d_{\mathrm{bo}}, T_{\mathrm{CAP}}/d_{\mathrm{bo}} + d_B/d_{\mathrm{bo}} - 1]$ and $j \in [0, T_{\mathrm{CAP}}/d_{\mathrm{bo}} - 1]$, and null otherwise, and

$$P\{Z^s\} = P\{Z^j\}_{\mathrm{CAP}} \cdot \frac{N - N_{\mathrm{GTS}}}{N} \tag{2}$$

for $s \in [d_B/d_{\mathrm{bo}}, T_{\mathrm{CAP}}/d_{\mathrm{bo}} + d_B/d_{\mathrm{bo}} - 1]$ and $j \in [0, T_{\mathrm{CAP}}/d_{\mathrm{bo}} - 1]$, and null otherwise.

In the CFP, $P\{T^s\} = P\{Z^s\} = 1/N$ for $s = T_{\mathrm{CAP}}/d_{\mathrm{bo}} + d_B/d_{\mathrm{bo}} + k \cdot D_{\mathrm{GTS}} \cdot 3 \cdot 2^{SO} + D - 1$, with $k \in [0, N_{\mathrm{GTS}} - 1]$,

TABLE I
DEFINITION OF VARIABLES

N	Number of nodes in the network
N_{GTS}	Number of GTSs allocated
T_B	Beacon Interval
T_A	Superframe duration
T_s	Symbol time
T_{CAP}	CAP duration
d_B	Beacon duration
d_{GTS}	Duration of a GTS
d_{bo}	Backoff period duration
d_{ifs}	Inter-frame space duration
$P\{T^s\}$	Prob. a node ends tx in slot s
$P\{Z^s\}$	Prob. coord. rx packet tail in slot s
p_s	Success probability
$P\{T^j\}_{CAP}$	Prob. a node ends tx in slot j in the CAP
$P\{Z^j\}_{CAP}$	Prob. coord. rx packet tail in slot j in the CAP
$p_{s_{CAP}}$	Success probability in the CAP
b_w^j	Prob. to find the channel busy when $CW = w$, at slot j
f^j	Prob. to find the channel free in slots $j-1$ and j
D	Number of backoff periods occupied by a packet
S	Throughput
G	Offered traffic
D_{mean}	Average delay
z	Data packet size
z_B	Beacon packet size

and null otherwise. Recall that transmissions are referred to the last slot in which the transmission occurs and that no collisions happen in GTSs.

We can also evaluate the cumulative functions $F_T(s)$ and $F_Z(s)$, which is defined as the probability that a node transmits its packet within slot s and that a node transmits correctly its packet within s, respectively, given by $F_T(s) = \sum_{v=0}^{s} P\{T^v\}$ and $F_Z(s) = \sum_{v=0}^{s} P\{Z^v\}$.

The success probability p_s for a packet transmitted by a node in a network composed of N nodes organized in a star topology is

$$p_s(N) = p_{s_{\mathrm{CAP}}}(N - N_{\mathrm{GTS}}) \cdot \frac{N - N_{\mathrm{GTS}}}{N} + \frac{N_{\mathrm{GTS}}}{N} \qquad (3)$$

where $p_{s_{\mathrm{CAP}}}(N - N_{\mathrm{GTS}})$ is the success probability for a packet transmitted in the CAP portion, through the CSMA/CA algorithm, when $N - N_{\mathrm{GTS}}$ nodes compete for the channel. The success probability for a packet transmitted in the CFP, instead, is equal to one.

Finally, the average delay D_{mean} is given by

$$D_{\mathrm{mean}} = d_{\mathrm{bo}} \cdot \sum_{s=0}^{T_A/d_{\mathrm{bo}}-1} (s+1) \frac{P\{Z^s\}}{p_s} \qquad (4)$$

where $s+1$ is the delay, in backoff periods, of a packet correctly received in slot s, and $P\{Z^s\}/p_s$ is the probability that the packet tail is received in slot s, given that the packet has been correctly received.

The probabilities $P\{T^j\}_{\mathrm{CAP}}$, $P\{Z^j\}_{\mathrm{CAP}}$, and $p_{s_{\mathrm{CAP}}}$, which are related to the CAP portion, are derived in the following sections, where the mathematical model of the CSMA/CA algorithm is introduced.

For the sake of clarity, the list of variables used in this paper is provided in Table I.

TABLE II
BACKOFF STAGES

BO_s	NB	BE	$W_{NB} = 2^{BE}$
0	0	BE_{min}	$W_0 = 2^{BE_{min}}$
1	1	$BE_{min}+1$	$W_1 = 2^{BE_{min}+1}$
..	..	..	..
NB_{max}	NB_{max}	BE_{max}	$W_{NB_{max}} = 2^{BE_{max}}$

VI. FORMULATION OF THE MATHEMATICAL MODEL FOR THE CAP

A. Node States

Generally speaking, a node accessing the channel during the CAP portion of the superframe can be in one of the following four states: 1) backoff; 2) sensing; 3) transmission; and 4) idle. However, if after sensing, the channel is free for two subsequent slots, transmission immediately occurs, followed by a sequence of idle states until the end of the superframe. Thus, given the objectives of this paper, we need to model only the backoff and sensing states.

The node state is modeled as a 3-D process $Q(\hat{t}) = \{BO_c(\hat{t}), BO_s(\hat{t}), CW(\hat{t})\}$, where $\hat{t}$ is an integer, representing the time, expressed in number of slots, having set the origin of this time axis ($\hat{t} = 0$) at the instant in which nodes receive the beacon. Therefore, $\hat{t} = j$ denotes the jth slot (from $j \cdot d_{\mathrm{bo}}$ to $(j+1) \cdot d_{\mathrm{bo}}$), after the reception of the beacon, i.e., the interval of time between $d_B + j \cdot d_{\mathrm{bo}}$ and $d_B + (j+1) \cdot d_{\mathrm{bo}}$.

$BO_c(\hat{t})$ and $BO_s(\hat{t})$ represent the backoff time counter and the backoff stage at time $\hat{t}$, respectively, and $CW(\hat{t})$ is the value of CW at time $\hat{t}$. $BO_c(\hat{t})$ counts the number of slots a node must wait before sensing the channel, whereas $BO_s(\hat{t})$ dimensions the maximum duration of the backoff phase. $BO_c(\hat{t})$ and $BO_s(\hat{t})$ are time-discrete stochastic processes assuming discrete values. Therefore, the process is a chain; however, it is not a Markovian chain [22] because $BO_c(\hat{t})$ is not a memoryless process as its value depends on its history.

The initial value of the backoff time counter $(BO_c(0))$ is uniformly distributed in the range $[0, W_{NB} - 1]$, where $W_{NB} = 2^{BE}$ is the dimension of the contention window, and $NB \in [0, NB_{\max}]$. The value of BE depends on the second process characterizing the state: $BO_s(t)$. We can identify $NB_{\max} + 1$ different backoff stages obtained by considering the different possible combinations of the pair (NB, BE). In Table II, the different backoff stages with the corresponding W_{NB} values (denoted as $W_0, \ldots, W_{NB_{\max}}$) are shown.

The 802.15.4 MAC protocol states that at the beginning of the backoff algorithm, each node sets $NB = 0$ and $BE = BE_{\min}$. Then, each time the channel is sensed busy, NB and BE are increased by 1. When BE reaches its maximum value, there is no more increase. The case $BO_s = NB_{\max}$ is the last case, because here, NB reaches its maximum value, and it cannot be further increased.

Since there exists a maximum value for NB, there will also be a maximum delay affecting the transmission of a packet. This maximum is reached in case a node extracts at every backoff stage the higher backoff time counter and at the end of each backoff stage it always finds the channel busy. Therefore, the last slot in which a transmission can start is $\hat{t}_{\max} = \sum_{k=0}^{NB_{\max}} W_k + k + 1$, and the last slot in which a transmission can finish is $(\hat{t}_{\max} + D - 1)$.

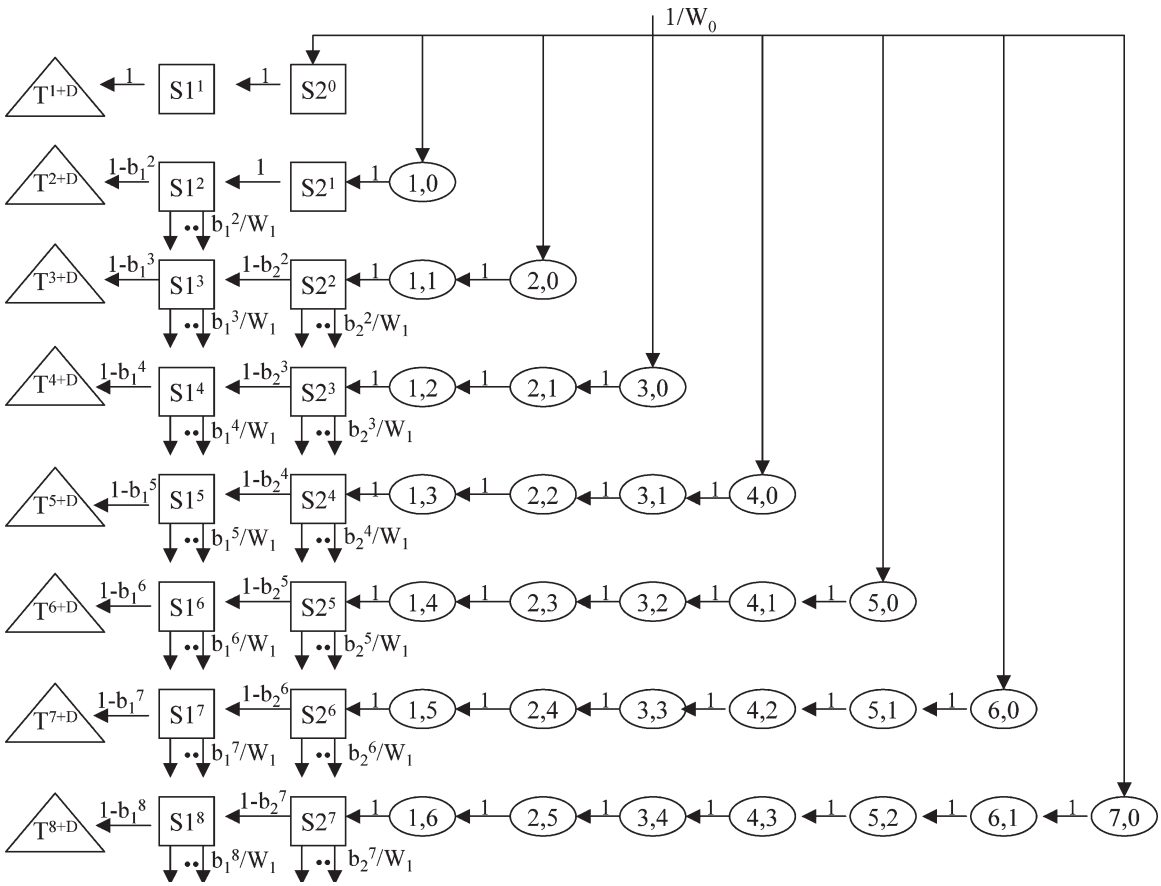

Fig. 3. State–transition diagram of the first backoff stage.

In the following, the generic state will be denoted as $Q(\hat{t}) = \{BO_c, BO_s, CW, \hat{t}\}$, and the probability of being in a generic state will be denoted as $P\{BO_c = c, BO_s = i, CW = w, \hat{t} = j\} = P\{c, i, w, j\}$. In particular, the probability of being in a backoff state will be denoted as $P\{c, i, 2, j\}$ since in these states, CW is equal to 2, whereas the probability of being in the first sensing phase (i.e., when $CW = 2$) and in the second sensing phase (i.e., when $CW = 1$) at the jth slot and in the ith backoff stage will be denoted as $P\{S2_i^j\} = P\{0, i, 2, j\}$ and $P\{S1_i^j\} = P\{0, i, 1, j\}$, respectively. Note that when a node is in sensing, BO_c is equal to zero.

B. Steps Followed by the Model

Let us denote as b_w^j the probability that in the jth slot, when $CW = w$, the channel is found busy after sensing. Since CW is equal to 2 when a node performs the first sensing phase and to 1 when it performs the second sensing phase, we will denote as b_2^j the probability of finding the channel busy in the first phase and as b_1^j the probability of finding the channel busy in the second phase. Finally, we will denote as f^j, the joint probability of finding the channel free in slots j and $j-1$ (i.e., the probability that a node starting sensing in slot $j-1$ finds the channel free for two subsequent slots). These probabilities will be initially left as parameters, and their computation will be performed in Section VII-C. The model provides $P\{T^j\}_{\mathrm{CAP}}$ and $P\{Z^j\}_{\mathrm{CAP}}$, with $j \in [0, T_{\mathrm{CAP}}/d_{\mathrm{bo}} - 1]$ and $p_{s_{\mathrm{CAP}}}$.

The probability $P\{T^j\}_{\mathrm{CAP}}$ depends on the probability of being in the sensing state in slot $j - D - 1$ (since a packet occupies D slots) and on finding the channel free for two subsequent slots. To determine the sensing probabilities, we model the behavior of a single node using a state–transition diagram [22], describing the relation between all possible states in which a node can be (see below). From this diagram, we obtain the probabilities $P\{S1_i^j\}$ and $P\{S2_i^j\}$, whatever j and i are. This is made in the remainder of this section. From these probabilities, we can derive the probabilities $P\{T^j\}_{\mathrm{CAP}}$ (see Section VII-A). The probabilities $P\{Z^j\}_{\mathrm{CAP}}$ and $p_{s_{\mathrm{CAP}}}$, instead, are derived in Section VII-B. Section VII-C gives b_1^j, b_2^j, and f^j.

C. Sensing Probabilities

The state–transition diagram of the 3-D process $Q(\hat{t})$ is presented through different figures—one for each backoff stage. The part of the diagram related to the first backoff stage $(BO_s = 0)$, which is obtained when the MAC parameters are set to the default values ($BE_{\min} = 3$, $BE_{\max} = 5$, $NB_{\max} = 4$), is reported in Fig. 3 and commented in this section. The part of the diagram related to the generic backoff stage $(BO_s = k)$ is, instead, reported in Figs. 13 and 14 and commented upon in the Appendix.

As will be clarified in the following, the different figures are linked together through transitions that originate from some states of a figure and terminate in the states of the figure related to the following backoff stage. Because each figure is related

to a specific value of BO_s, for the sake of simplicity in the drawings, the generic backoff state (ovals in the figures) is simply denoted as $\{c, j\}$, omitting the value of BO_s, as well as the value of CW, which is equal to 2 for all the backoff states. The sensing states (squares) are denoted as $S1^j$ and $S2^j$ with no pedex i. Finally, the transmission states (triangles in the figures) are denoted as T^j, with no pedex i.

In the following, the part of the diagram related to the first backoff stage is described. The probabilities of being in the different states of the chain and the transition probabilities between the states are provided.

At the beginning of the backoff algorithm, each node extracts an integer, uniformly distributed between 0 and $W_0 - 1$. At $\hat{t} = 0$ a node enters, with probability $1/W_0$, one of the states $\{c, 0, 2, 0\}$, with $c \in [0, W_0 - 1]$. If the extracted value is 0, the node in slots 0 and 1 will sense the channel, and in slot 2, it will transmit its packet because no transmission may occur in the first two slots, and therefore, the channel will certainly be found free ($f^1 = 1$). In the case where a value larger than 0 is extracted, the node will decrease its backoff counter at each slot until the counter will reach the zero value when the node will start sensing. In case the channel is found free for two subsequent slots, the node will transmit the packet; otherwise, it will pass to the following backoff stage, and another value, which is uniformly distributed between 0 and $W_1 - 1$, will be extracted. In Fig. 3, the transitions that originated from the sensing states enter the states of part of the diagram related to $BO_s = 1$, as shown in Fig. 13, once we set $k = 1$. For example, if a node is in state $S2_0^1$ and it finds the channel busy, it will enter state $S2_1^2$, or one of the states $\{c, 1, 2, 2\}$, with $c \in [1, W_1 - 1]$, with the same probability b_2^1/W_1. The state of arrival depends on the new backoff counter value extracted.

Denoting as $P\{BO_c = c_1, BO_s = i_1, CW = w_1, \hat{t} = j_1 | BO_c = c_0, BO_s = i_0, CW = w_0, \hat{t} = j_0\} = P\{c_1, i_1, w_1, j_1 | c_0, i_0, w_0, j_0\}$ the transition probability from the state $\{c_0, i_0, w_0, j_0\}$ to the state $\{c_1, i_1, w_1, j_1\}$, the transition probabilities between the backoff states are given by

$$P\{c, 0, 2, j + 1 | c + 1, 0, 2, j\} = 1 \tag{5}$$

for $c \in [0, W_0 - 2]$ and $j \in [0, W_0 - 2]$. This equation accounts for the fact that at the beginning of each time slot, the backoff time counter is decreased by 1 until it reaches the zero value, with a probability of 1.

The probabilities of being in a sensing state when $CW = 2$ are given by

$$P\left\{S2_0^j\right\} = \begin{cases} \frac{1}{W_0}, & \text{for } j \in [0, W_0 - 1] \\ 0, & \text{otherwise.} \end{cases} \tag{6}$$

The probabilities of being in a sensing state when $CW = 1$ are given by

$$P\left\{S1_0^j\right\} = \begin{cases} P\left\{S2_0^{j-1}\right\} \cdot \left(1 - b_2^{j-1}\right), & \text{for } j \in [1, W_0] \\ 0, & \text{otherwise.} \end{cases} \tag{7}$$

A node, in fact, will sense the channel for the second time if and only if it finds the channel free during the first sensing phase.

Similar formulas are achieved for the other backoff stages and are reported in the Appendix.

VII. Performance Evaluation for the CAP

A. Transmission Probabilities

As stated before, the aim of the model is to evaluate the probability that a generic node ends its packet transmission in slot j, $P\{T^j\}_{\mathrm{CAP}}$, with $j \in [0, T_{\mathrm{CAP}}/d_{\mathrm{bo}} - 1]$.

A node finishes its transmission in slot j if in slot $j - D - 1$, it starts sensing the channel finding it free for two subsequent slots. The probability that a node starts sensing in slot j is the sum of the probabilities of starting sensing in the jth slot and at the ith backoff stage, considering all the possible backoff stages. Therefore, we obtain

$$P\{T^j\}_{\mathrm{CAP}} = f^{j-D} \cdot \sum_{k=0}^{NB_{\max}} P\left\{S2_k^{j-D-1}\right\} \tag{8}$$

for $j \in [D + 1, \hat{t}_{\max} + D - 1]$, and null otherwise. Because a node transmits a packet occupying D slots, we associate $P\{T^j\}_{\mathrm{CAP}}$ with the slot in which the transmission terminates.

$P\{T^j\}_{\mathrm{CAP}}$ given by (8) is substituted in (1) to derive the statistics in the whole superframe.

B. Success Probability

To evaluate the other target probabilities, we have to model how the number of nodes that compete for the channel varies with time. We denote as N_c^j the number of nodes that have yet to transmit at the end of slot $j - 1$ and will compete for slot j. By passing time, some nodes in the network may access the channel; therefore, N_c^j decreases by increasing j. In particular, as shown in [14], N_c^j is a random variable that is binomially distributed. However, a precise evaluation of the statistics of this variable is complex from the computational viewpoint since it depends on the statistics of N_c^{j-1} whose determination would depend on the statistics of N_c^{j-2}, and so on. To reduce such complexity, in [14], different approximations have been introduced, and compared. Results show that these approximations bring approximately the same results; therefore, here, we use the simplest approximation, according to which we set $N_c^j = N_c$, whatever j is. In the case of star topologies, N_c is the number of nodes using the CAP; therefore $N - N_{\mathrm{GTS}}$. In Section IX, simulations are compared with the mathematical approach. Results show that very good agreement with simulations is obtained through the model, despite the approximation introduced. In fact, when N is large, N_c^j slowly decreases, and the approximation is good. When, instead, the offered traffic is small, the decrease in N_c^j is more notable, but the probabilities of finding the channel busy and colliding are small since few nodes are competing for the channel. Therefore, these probabilities are not strongly affected by the decrease in N_c^j.

The probability $p_{s_{\mathrm{CAP}}}$ that a generic packet is transmitted successfully on the channel is given by

$$p_{s_{\mathrm{CAP}}} = \begin{cases} \sum_{j=0}^{\hat{t}_{\max}+D-1} P\{Z^j\}_{\mathrm{CAP}}, & \text{if } \hat{t}_{\max}+D-1 \\ & \quad \le T_{\mathrm{CAP}}/d_{\mathrm{bo}}-1 \\ \sum_{j=0}^{T_{\mathrm{CAP}}/d_{\mathrm{bo}}-1} P\{Z^j\}_{\mathrm{CAP}}, & \text{otherwise} \end{cases} \tag{9}$$

where $P\{Z^j\}_{\mathrm{CAP}}$ is the probability that a successful transmission ends in slot j, which means that one and only one transmission starts in $j-D+1$.

As only one transmission starts in slot $j-D+1$ if only one node, over N_c, senses the channel in slot $j-D$ and if the channel is free in $j-D$ and $j-D-1$, $P\{Z^j\}_{\mathrm{CAP}}$ is given by

$$P\{Z^j\}_{\mathrm{CAP}} = f^{j-D} \cdot \sum_{k=0}^{NB_{\max}} P\left\{S2_k^{j-D-1}\right\} \cdot \prod_{k=0}^{NB_{\max}} \left(1-P\left\{S2_k^{j-D-1}\right\}\right)^{N_c-1} \quad (10)$$

where the second factor gives the probability that one node senses the channel in $j-D-1$, whatever the backoff stage, and the third factor gives the probability that the remaining N_c-1 nodes do not sense the channel in slot $j-D-1$.

C. Probability of Finding the Channel Busy

The channel will be found busy in slot j in case a transmission starts in slot j, or in slot $j-1$, up to slot $j-D+1$, since each node transmits a packet occupying D slots. Therefore, by denoting as $P\{T_1^j\}$ the probability that at least one transmission starts in slot j, the probability of finding the channel busy during the first sensing phase $(CW=2)$ is given by

$$b_2^j = \sum_{v=j-D+1}^{j} P\{T_1^v\} \quad (11)$$

whereas b_1^j is the probability of finding the channel busy, conditioned on the fact that the channel in $j-1$ was free since a node performs the second sensing phase only if it has found the channel free in the first slot. Therefore, it is the probability that slot $j-2$ is free and that there is at least one node starting sensing in this slot. We have

$$b_1^j = \left(1-b_2^{j-2}\right) \cdot \left[1-\prod_{k=0}^{NB_{\max}} \left(1-P\left\{S2_k^{j-2}\right\}\right)^{N_c-1}\right] \quad (12)$$

where the second factor (between the brackets) is the probability that at least one node starts sensing in slot $j-2$.

The channel will be jointly free in slots j and $j-1$ if no transmissions start in slots j, $j-1$, up to $j-D$, and therefore, the probability f^j is given by

$$f^j = 1 - \sum_{v=j-D}^{j} P\{T_1^v\}. \quad (13)$$

Finally, the probability that at least one transmission starts in slot j is given by

$$P\left\{T_1^j\right\} = f^{j-1} \cdot \left[1-\prod_{k=0}^{NB_{\max}} \left(1-P\left\{S2_k^{j-2}\right\}\right)^{N_c-1}\right]. \quad (14)$$

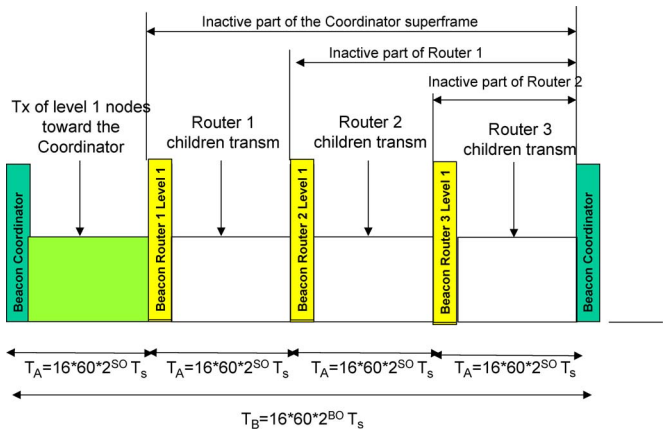

Fig. 4. Superframe structure used in the tree-based topology.

VIII. Tree-Based Topology

As stated above, when the number of nodes in the PAN gets larger, star topologies are not suitable and peer-to-peer or tree-based topologies should be used [2], [23]. An L-level tree rooted at the PAN coordinator (namely, at level zero) is considered. Level i nodes receive data from level $i+1$ nodes and forward them to level $i-1$ nodes toward the coordinator. The tree-based topology defined by Zigbee Alliance [2] is accounted for.

According to the Zigbee specifications, the tree formation procedure is started by the PAN coordinator, which broadcasts beacons to nodes. A candidate node receiving the beacon may request to join the network at the coordinator. If the coordinator allows the node to join, it will start transmitting beacons to allow other candidate nodes to join the network.

Nodes work in beacon-enabled mode: Each child node tracks the beacon of its parent and transmits its own beacon at a predefined offset with respect to the beginning of its parent beacon. The offset must always be larger than the parent superframe duration and smaller than beacon interval. This implies that the beacon and the active part of child superframe reside in the inactive period of the parent superframe: No overlap between the active portions of the superframes of child and parent is present (see Fig. 4 as an example). This concept can be expanded to cover more than two nodes: The selected offset must not result in beacon collisions with neighboring nodes. Obviously, a child will transmit a beacon packet only in case it is a router. Each child will transmit its packet to the parent in the active part (CAP or CFP) of the parent superframe.

We set the duration of all the active parts of the superframes generated by the routers and by the coordinator at the same value (i.e., we set a unique value of SO). Under these conditions, once we set the BO value, the number of routers (including the coordinator) that will have a portion of superframe available to receive data from their children will be equal to 2^{BO-SO} (see Fig. 4). If the number of routers in the network is larger than 2^{BO-SO}, some routers will not have a portion of superframe available, their children will not be able to access the channel, and their packets will be lost. We denote as p_{frame_i} the probability that a level i router has a portion of superframe allocated in which it can receive data from its children.

We denote as p_i the probability that a node is at level i of the hierarchy and with $p_s(n_i)$ the success probability for a level i node competing for the channel with the other $n_i - 1$ nodes connected to the same parent at level $i-1$. A packet coming from a level i node will be correctly received by the coordinator, in case it is successfully transmitted by the level i node from which it is generated and by all the routers from level $i-1$ until level one, forwarding it toward the coordinator. The success probability for a node accessing the channel in the tree is therefore

$$p_{s_{\text{tree}}} = \sum_{i=1}^{L-1} p_i \cdot p_{\text{frame}_{i-1}} \cdot \prod_{k=1}^{i} \overline{p_{s_k}} \tag{15}$$

where $\overline{p_{s_k}}$ is the average success probability for a node at level k, which is given by

$$\overline{p_{s_k}} = \sum_{n_k=0}^{N_k} p_s(n_k) \cdot \text{Prob}\{n_k\} \tag{16}$$

where $\text{Prob}\{n_k\}$ is the probability of having n_k nodes at level k connected to the same parent at level $k-1$, and N_k is the total number of nodes at level k. According to the channel access strategy defined above, only the children of a given parent compete for the channel; therefore, the tree could be seen as a series of stars, each having a parent and its children, operating independently (i.e., without collisions). Therefore, $p_s(n_k)$ is given by (3), by simply setting $N = n_k$, whereas $\text{Prob}\{n_k\}$ depends on the strategy used to form the tree.

Note that (15) could be used to evaluate the success probability for a node accessing the channel when a L-level tree-based topology is established, regardless of the strategy used to realize the tree.

Now, the success probability $p_{s_{\text{tree}}}$ is evaluated in the particular case of a three-level tree ($L = 3$). We denote as $N_i = p_i \cdot N$ the number of level i nodes. We assume that each level one router performs data aggregation: The received packets are aggregated to that generated by the router itself, resulting in a packet of the same size of the single aggregated packets. We also assume that level two nodes select randomly the level one parent and that the active part of the coordinator superframe is used by level one nodes to transmit toward the PAN coordinator. The remaining $2^{BO-SO} - 1$ superframe portions are randomly allocated to level one routers for receiving data from their children. Under these assumptions we will have $p_{\text{frame}_0} = 1$, whereas the probability that a level one router does not have a portion of the superframe available, p_{frame_1}, will be given by

$$p_{\text{frame}_1} = \frac{2^{BO-SO} - 1}{N_R} \tag{17}$$

where N_R is the mean number of level one routers, i.e., the number of level one nodes with at least one child, which is given by

$$N_R = \sum_{i=0}^{N_1} \binom{N_1}{i} (p_{\text{child}})^i \cdot (1 - p_{\text{child}})^{N_1 - i} \tag{18}$$

where $p_{\text{child}} = 1 - (1 - (1/N_1))^{N_2}$ is the probability that a level one node has at least a child, and $1/N_1$ is the probability that a level two node is connected to a given level one node.

Since level two nodes randomly select level one nodes to which transmit, the number of level two nodes connected to the same level one node will be binomially distributed. We have

$$\text{Prob}\{n_2 = i\} = \binom{N_2}{i} \left(\frac{1}{N_1}\right)^i \cdot \left(1 - \frac{1}{N_1}\right)^{N_2 - i}. \tag{19}$$

Therefore, the average success probability for a node being at level two will be

$$\overline{p_{s_2}} = \sum_{i=0}^{N_2} p_s(i) \cdot \binom{N_2}{i} \left(\frac{1}{N_1}\right)^i \cdot \left(1 - \frac{1}{N_1}\right)^{N_2 - i} \tag{20}$$

where $p_s(i)$ is the success probability given by (3) when i nodes at level two are competing for transmitting to the same level one node. Finally, according to (15), we achieve

$$p_{s_{\text{tree}}} = p_1 \cdot \overline{p_{s_1}} + p_2 \cdot p_{\text{frame}_1} \cdot \overline{p_{s_1}} \cdot \overline{p_{s_2}} \tag{21}$$

where p_{frame_1} is given by (17), and $\overline{p_{s_1}} = p_s(N_1)$.

The average delay, denoted as $D_{\text{mean}_{\text{tree}}}$ in the case of a tree, depends on the average delays of the packets coming from level one and level two nodes, denoted as D_{mean_1} and D_{mean_2}, respectively.

As stated above, level one nodes use the first portion of the superframe defined by the coordinator to transmit packets (see Fig. 4). Since these nodes could be seen as nodes of a star topology transmitting their packets directly to the coordinator, according to (4), we obtain

$$D_{\text{mean}_1} = d_{\text{bo}} \cdot \sum_{s=0}^{T_A/d_{\text{bo}}-1} (s+1) \frac{P\{Z^s\}(N_1)}{p_s(N_1)} \tag{22}$$

where $P\{Z^s\}(N_1)/p_s(N_1)$ is the probability that the packet tail is correctly received by the coordinator in slot s when N_1 nodes compete for the channel, given that the packet is correctly received. T_A is the duration of the active part of the superframe defined by the coordinator.

A packet coming from a level two node, instead, must be transmitted toward the level one parent and then from the latter to the coordinator. Therefore, two superframes are needed—one for each hop. Level one routers, in fact, always transmit to the coordinator the packets received by their children in the previous superframe. Therefore, the total average delay suffered by a level two node packet will be equal to T_B plus the average delay of its parent (i.e., the average delay of a level one node packet): $D_{\text{mean}_2} = D_{\text{mean}_1} + T_B$. Note that D_{mean_2} does not depend on the instant at which the parent receives the packet within its superframe.

Finally, the average delay suffered by a packet coming from whatever a node in a tree is given by

$$D_{\text{mean}_{\text{tree}}} = p_1 \cdot D_{\text{mean}_1} + p_2 \cdot D_{\text{mean}_2}. \tag{23}$$

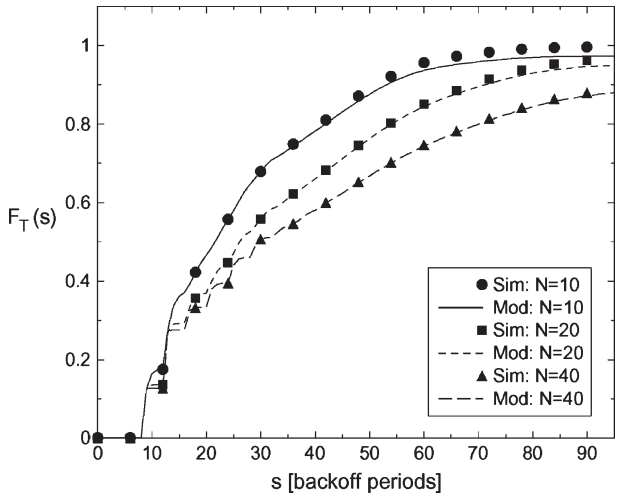

Fig. 5. Cumulative function $F_T(s)$ when $N_{\rm GTS} = 0$ and $D = 2$.

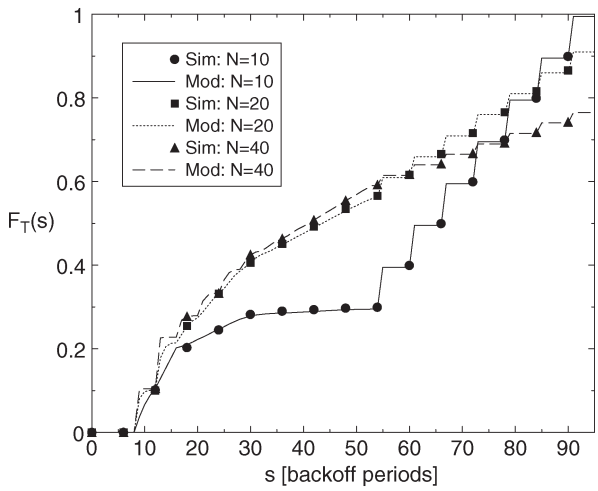

Fig. 6. Cumulative function $F_T(s)$ when $N_{\rm GTS} = 7$ and $D = 2$.

IX. Numerical Results

A. Star Topology

For the purpose of numerical comparison, a dedicated simulation tool written in the C language has been developed. The simulator generates a network composed of N nodes and a PAN coordinator, sending beacons and waiting for the data from nodes. In case GTSs are used, the PAN coordinator randomly selects the $N_{\rm GTS}$ nodes to which GTSs are allocated, whereas the remaining nodes will use the CAP portion. According to the application scenario, nodes have only one packet per superframe to be transmitted, and when CAP is used, they start the CSMA/CA algorithm at the same time. The CSMA/CA protocol described in Section III is implemented. Ideal channel conditions are assumed; therefore, all nodes can "hear" each other and can correctly receive the query at each round. No capture effect is considered: in case two or more packets collide, they are all lost. Finally, no acknowledge and retransmission mechanisms are performed. We consider 10^4 transmissions in our simulator, which means that 10^4 queries and superframes are simulated.

In the following, we set $d_{\rm ifs} = 12\,T_s$ for the case $D = 2$ and $d_{\rm ifs} = 40\,T_s$ for the cases $D > 2$ and $z_B = 60$ bytes, assuming that a payload is present in the beacon packet.

In Figs. 5 and 6, the cumulative functions F_T, as a function of time s for different values of N, having set $D = 2$ when no GTSs and seven GTSs are allocated, are shown. Both mathematical (lines) and simulation (symbols) results are reported to validate the model: Excellent agreement between the two cases can be found in all cases. Results are obtained by setting $SO = 1$; therefore, $T_A = 30.72$ ms. There is no traffic toward the PAN coordinator in the first part of the superframe due to the transmission of the beacon and to the sensing phases. As expected, by increasing N, the delay with which a node accesses the channel increases. The curves do not reach the value 1 since some nodes do not succeed in accessing the channel by the end of the superframe. The stepwise behavior of curves is motivated by the move from one backoff stage to the following. $P\{T^j\}_{\rm CAP}$, in fact, presents relative maxima at the beginning of each backoff window (i.e., the interval of time in which transmissions of nodes performing the first, the second, etc., backoff stage, occur) and is approximately constant inside each backoff window [14].

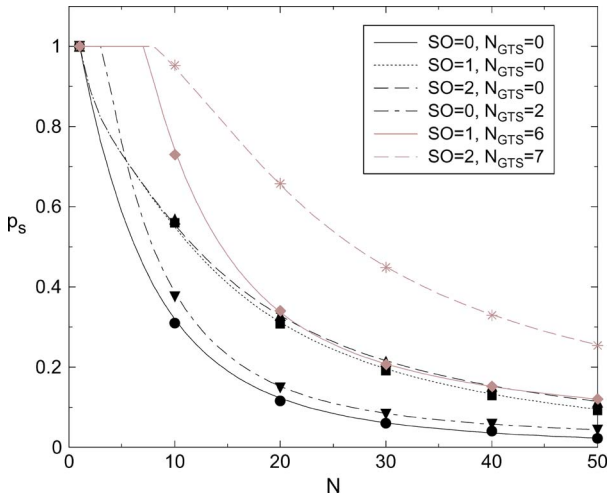

Fig. 7. Success probability p_s as a function of N when $D = 5$.

In Fig. 6, we can observe the statistics of the traffic in the CFP, characterized by steps in each GTS. With $d_{\rm ifs} = 12\,T_s$, we have $D_{\rm GTS} = 1$. The reason that the curves in the CAP portion of the superframe are down scaled with respect to those of Fig. 5 is that, here, the traffic in the CAP is due to the presence of $N - N_{\rm GTS}$ nodes instead of N. Moreover, nodes use the CAP only in the case where they do not have a GTS allocated (i.e., with probability $(N - N_{\rm GTS})/N$). For these reasons, the traffic in the CAP portion decreases.

In Fig. 7, p_s as a function of N, for different values of SO, having fixed $D = 5$, is shown. The cases of no GTSs and $N_{\rm GTS}$ equal to the maximum number of GTSs allocable are considered. As explained above, this maximum number depends on the values of D and SO. As we can see, p_s decreases monotonically (for $N > 1$ when $N_{\rm GTS} = 0$ and for $N > N_{\rm GTS}$ when $N_{\rm GTS} > 0$) by increasing N since the number of nodes competing for the channel increases. As expected, the use of GTSs improves performance since fewer nodes compete for the

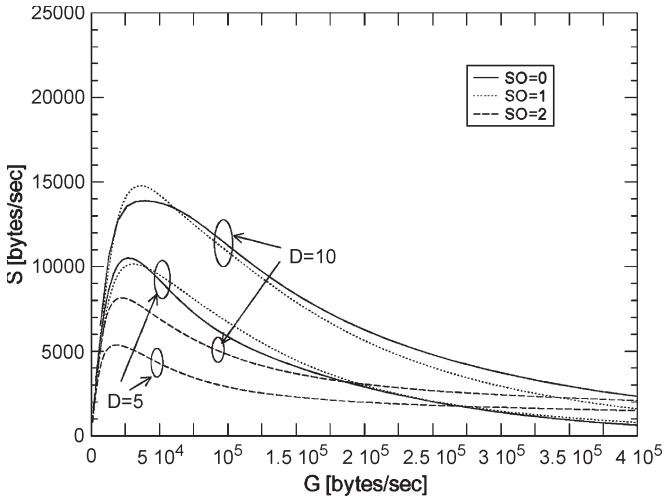

Fig. 8. Throughput S as a function of G when no GTSs are allocated.

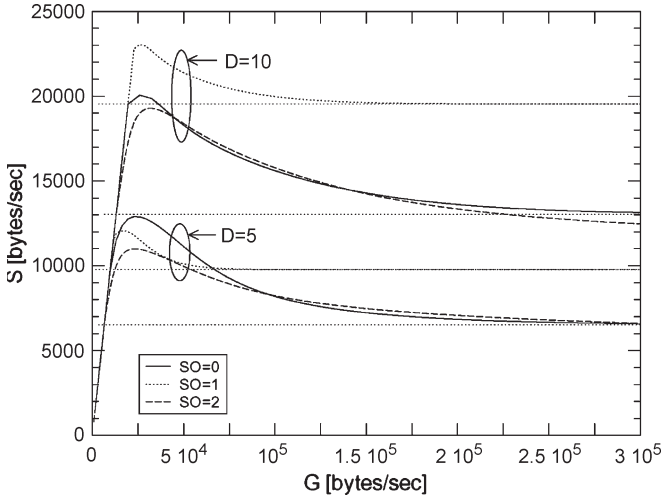

Fig. 9. Throughput S as a function of G when the maximum number of GTSs is allocated.

channel. By increasing SO, p_s gets larger since the CAP duration increases, and nodes have more time to access the channel.

Now, we introduce the concepts of throughput, denoted as S, and offered traffic, denoted as G. We define the throughput as the number of bytes per unit of time successfully transmitted to the coordinator, and the offered traffic as the maximum number of bytes the network was deployed to deliver per unit of time. G is given by

$$G = \frac{N \cdot z}{T_B} \text{ bytes/s} \tag{24}$$

whereas S is given by

$$\begin{aligned} S = p_s \cdot G &= \frac{N \cdot z}{T_B} \left(p_{s_{\text{CAP}}} \cdot \frac{N - N_{\text{GTS}}}{N} + \frac{N_{\text{GTS}}}{N} \right) \\ &= \frac{z}{T_B} \left[p_{s_{\text{CAP}}} \cdot (N - N_{\text{GTS}}) + N_{\text{GTS}} \right] \text{ bytes/s.} \end{aligned} \tag{25}$$

Bear in mind that $z = D \cdot 10$ bytes and $T_B = T_A$ (since $SO = BO$; see Section III) in the star topology case.

In Figs. 8 and 9, S as a function of G, when varying SO (i.e., T_A), and D, when no GTSs and when the maximum number of GTSs is allocated, are shown, respectively. When few nodes are

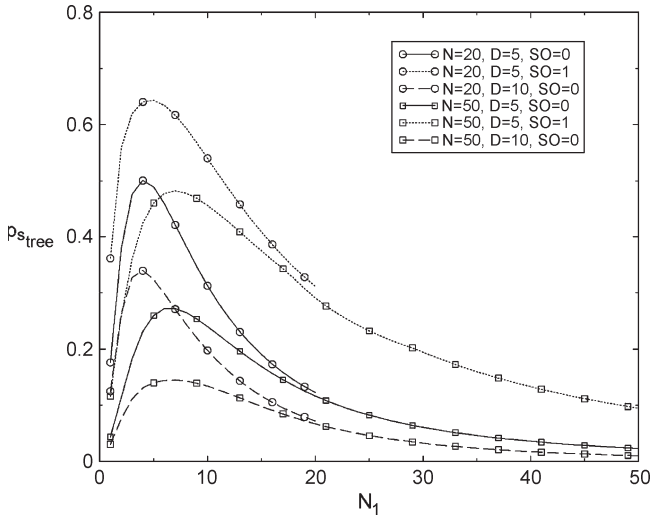

Fig. 10. $p_{s_{\text{tree}}}$ as a function of N_1 for the tree-based topology.

distributed in the network, by increasing G, S gets larger. With many nodes, an increase in G results in a decrease in S since many nodes are competing for the channel. This means that in star topologies, it is not convenient to increase N so much (i.e., the cost of the network) since many packets will be lost and that when N gets larger, star topologies are not suitable (this outcome was, in fact, expected). Moreover, we can note that there exists a value of SO maximizing S, which depends on G and D. As an example, for $D = 5$ when G is small, an increase in SO, even if p_s increases, results in a decrement of S since S also depends on $1/T_A$. When, instead, the offered traffic gets larger, collisions increase, and larger values of SO are required. On the other hand, when $D = 10$, the optimum value of SO is 1 for low G. This is due to the fact that having large packets, when $SO = 0$, too many packets are lost due to the short duration of the superframe.

When no GTSs are allocated (see Fig. 8), S decreases monotonically since $\lim_{G\to\infty} p_{s_{\text{CAP}}} = 0$. When, instead, GTSs are allocated (Fig. 9), there exists a horizontal asymptote, which is given by [by using (25)]

$$\lim_{G\to\infty} S = \frac{z \cdot N_{\text{GTS}}}{T_A}. \tag{26}$$

As an example, when $SO = 1$ and $D = 10$, the maximum number of GTSs that can be allocated is $N_{\text{GTS}} = 6$, and the horizontal asymptote is $S = 19531.25$ bytes/s.

B. Tree-Based Topology

Numerical results obtained in the three-level tree are discussed here and compared with results obtained in the star topology case. Since $p_{s_{\text{tree}}}$, $D_{\text{mean}_{\text{tree}}}$, and $P\{Z^s\}$ depend on p_s obtained in the star topology case that has been validated above, simulation results are not reported here.

In Fig. 10, $p_{s_{\text{tree}}}$ as a function of N_1, for different values of N, D, and SO, having set $BO = 5$, is shown. There exists an optimum value of N_1 maximizing $p_{s_{\text{tree}}}$, and this value obviously increases by increasing N and is approximately equal to $\sqrt{N}$; therefore, it is independent of D and SO. This means

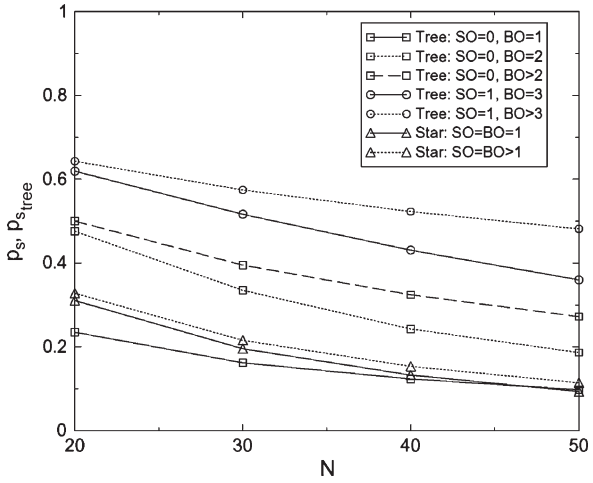

Fig. 11. Success probability as a function of N when "star" and tree-based topologies are used.

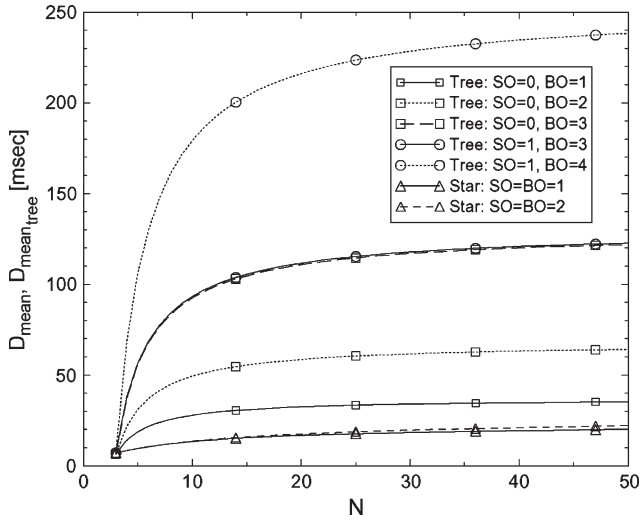

Fig. 12. Average delay as a function of N when star and tree-based topologies are used.

that, once we fix N, there exists an optimum split between level one and level two nodes, maximizing the probability of success.

In Fig. 11, results related to the two topologies, showing the success probability as a function of N for different values of SO and BO by setting $D = 5$, are compared. For a fair comparison, the success probability is computed by fixing the same value of T_B and, therefore, by giving to nodes the same time to transmit the data to the coordinator. To this aim, we set $SO = BO$ for the star topology, and we compare the case "star" with $SO = BO = 1$ with the case "tree," with $BO = 1$ and $SO = 0$, whereas the case "star" with $SO = BO > 1$ (note that the cases $SO = BO = 2, 3$, etc., bring the same p_s) are compared with the cases "tree" with $BO > 1$, whatever SO is. In the "tree" case, N_1 is set to the optimum value maximizing $p_{s_{\text{tree}}}$ obtained from Fig. 10. As we can see, when $BO = 1$, the "star" is preferable since in the "tree" only one router has a part of the superframe allocated; therefore, many packets of level two nodes are lost. For $BO > 1$, instead, the "tree" outperforms the "star." The difference between the "star" and the "tree" obviously increases by increasing BO and SO, resulting in an increase in p_{frame} and p_s, respectively.

In Fig. 12, the average delays obtained in case of star and tree-based topologies as a function of N are shown. The curves are obtained by setting $D = 5$ and $N_1 = 3$ in the case of trees. The delays increase by increasing N since the probability of finding the channel busy and delaying the transmission gets larger. A horizontal asymptote is also present due to the maximum delay that a packet may suffer, which is equal to the superframe duration T_A in the "star" case and to $T_B + T_A$ in the "tree" case. As expected, the delays are larger for trees since packets coming from level two nodes need two superframes to reach the coordinator. Also note that by increasing BO, delays get significantly larger. The curves "tree" with $SO = 0$, $BO = 3$ and "tree" with $SO = 1$ and $BO = 3$ overlapped since T_B assumes the same value and the delays of level one nodes are approximately the same (in fact, the curves "star" with $SO = BO = 0$ and $SO = BO = 1$ are also approximately the same).

By comparing Figs. 11 and 12, we can finally deduce that the choice of the topology depends on the application requirements: In case the application requires large success probability and it can tolerate large delays, trees are preferable. If, instead, more stringent constraints in terms of delays are imposed, star topologies are better. However, note that trees allow the realisation of larger networks distributed in wide areas, whereas the number of nodes that may directly reach the coordinator is limited by connectivity problems. However, the study of connectivity issues is out of the scope of this paper.

X. Conclusion

A mathematical model for the beacon-enabled mode of IEEE 802.15.4 has been provided. The model captures all aspects of the standard air interface, and it allows the evaluation of the statistical distribution of the traffic generated by nodes toward the PAN coordinator and of the probability that a node successfully transmits a packet. Results show how the distribution of the traffic, throughput, and probability of success changes when different loads are offered. The model is validated through a comparison with simulation results. A comparison between results obtained when star and tree-based topologies are considered is also provided. Results show that in terms of success probability, tree-based topologies are better in most cases but bring larger delays with respect to star topologies.

Appendix
Sensing Probabilities for $BO_s > 0$

We consider here the backoff stages $BO_s = 1, \ldots, NB_{\max}$, and we refer to the parts of the state transition diagram illustrated in Fig. 13 for the cases where $W_{0,\ldots,k-1} \leq W_k$ and in Fig. 14 for the cases where $W_{0,\ldots,k-1} > W_k$. Note that in the case of default MAC parameters ($BE_{\min} = 3$, $BE_{\max} = 5$, and $NB_{\max} = 4$), Fig. 13 refers to the cases $BO_s = 1$ and 2, and Fig. 14 shows the cases where $BO_s = 3$ and 4.

As in the case when $BO_s = 0$, the transition probabilities between backoff states in the kth backoff stage are given by

$$P\{c, k, 2, j+1 | c+1, k, 2, j\} = 1 \tag{27}$$

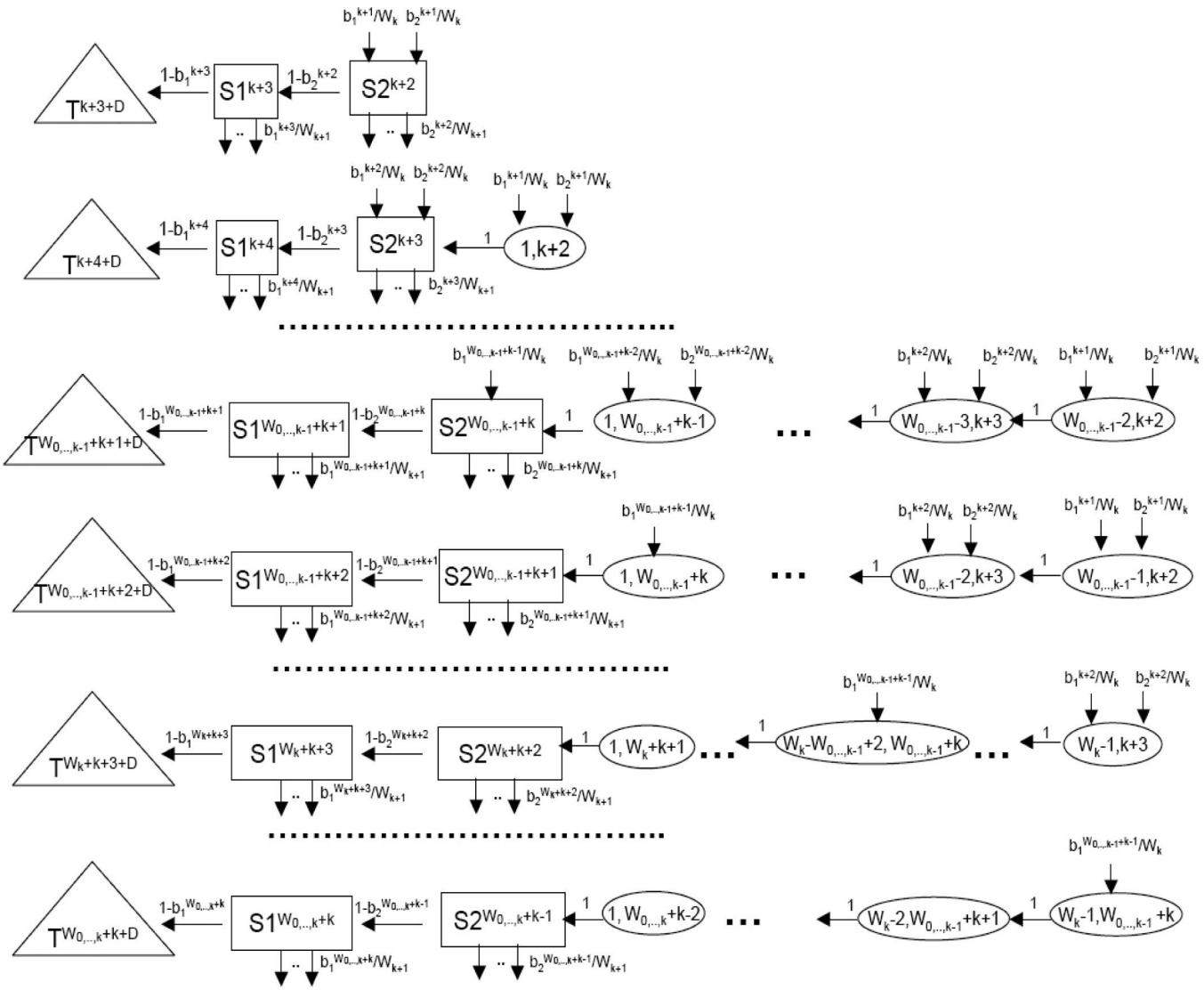

Fig. 13. State–transition diagram of the kth backoff stage in the case where $W_{0,\dots,k-1} \leq W_k$.

for $c \in [0, W_k - 2]$ and $j \in [k+2, W_{0,1,\dots,k} + k - 2]$, where $W_{0,1,\dots,k} = W_0 + W_1 + \cdots + W_k$. In the following, we will denote as $W_{x,y,z}$ the sum $W_x + W_y + W_z$.

The transition probabilities between the sensing states at $CW = 2$ of the backoff stage k and those of the backoff stage $k+1$ are given by

$$P\{c, k, 2, j+1 | 0, k-1, 2, j\} = \frac{b_2^j}{W_k} \tag{28}$$

for $c \in [0, W_k - 1]$ and $j \in [k+1, W_{k-1} + k - 2]$. This equation accounts for the fact that in case a node is in the $k-1$th backoff stage and the channel at slot j is found busy, the node will reach one of the states $\{c, k, 2, j+1\}$, with $c \in [0, W_k - 1]$ and with the same probability $1/W_k$.

The transition probabilities between the sensing states of two subsequent backoff stages when $CW = 1$ are given by

$$P\{c, k, 2, j+1 | 0, k-1, 1, j\} = \frac{b_1^j}{W_k} \tag{29}$$

for $c \in [0, W_k - 1]$ and $j \in [k+1, W_{k-1} + k - 1]$.

If $W_{0,\dots,k-1} \leq W_k$ (see Fig. 13), the probabilities of being in sensing when $CW = 2$ are given in (30), shown at the bottom of the page.

$$P\left\{S2_k^j\right\} = \begin{cases} \sum_{v=k+1}^{j-1} \left(P\left\{S1_{k-1}^v\right\} \cdot \frac{b_1^v}{W_k} + P\left\{S2_{k-1}^v\right\} \cdot \frac{b_2^v}{W_k} \right), & \text{for } j \in [k+2, W_{0,\dots,k-1} + k] \\ P\left\{S2_k^{W_{0,\dots,k-1}+k}\right\}, & \text{for } j \in [W_{0,\dots,k-1} + k + 1, W_k + k + 1] \\ \sum_{v=j-W_k}^{W_{0,\dots,k-1}+k-1} \left(P\left\{S1_{k-1}^v\right\} \cdot \frac{b_1^v}{W_k} + P\left\{S2_{k-1}^v\right\} \cdot \frac{b_2^v}{W_k} \right), & \text{for } j \in [W_k + k + 2, W_{0,\dots,k} + k - 1] \\ 0, & \text{otherwise} \end{cases} \tag{30}$$

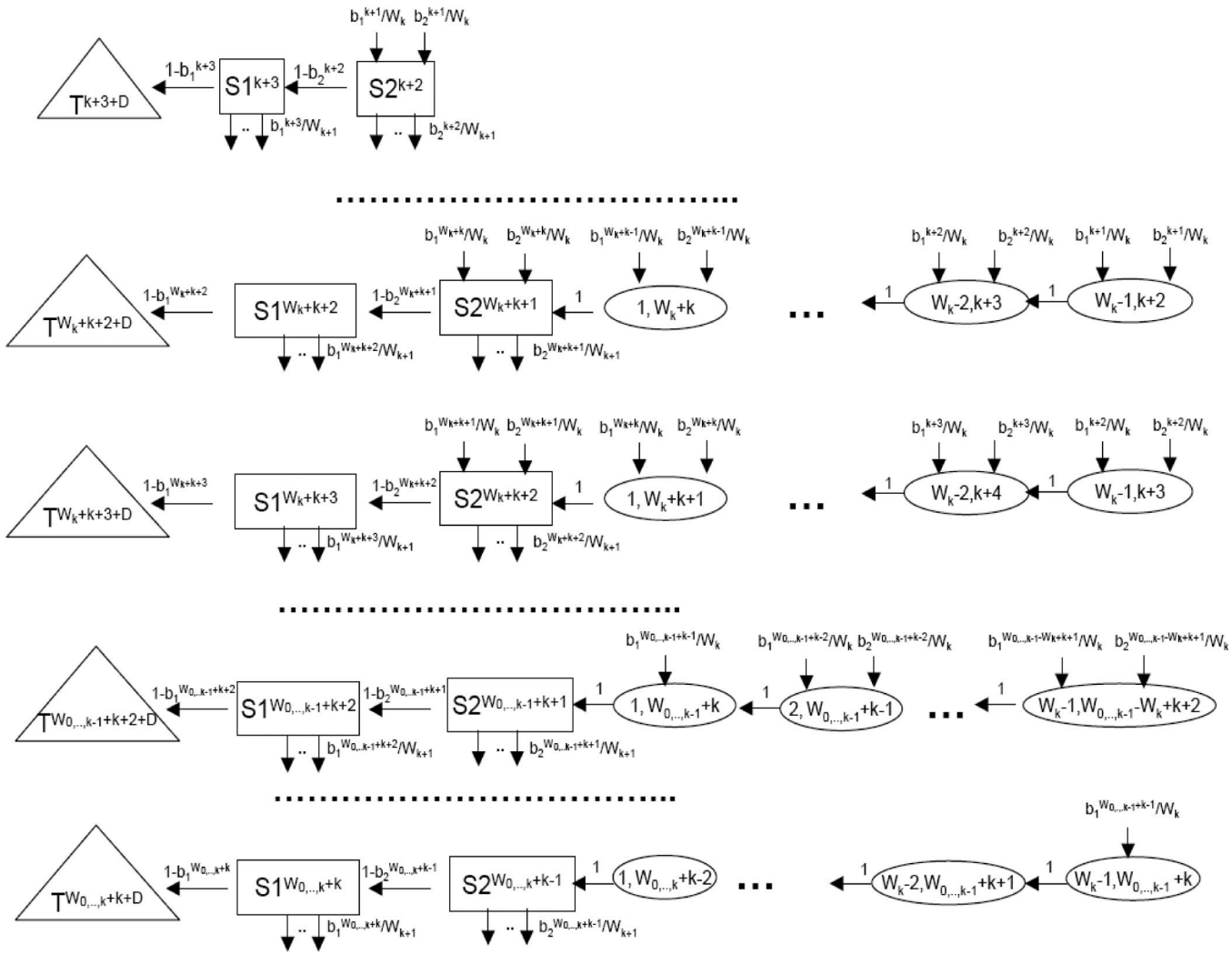

Fig. 14. State–transition diagram of the kth backoff stage in the case where $W_{0,\ldots,k-1} > W_k$.

Let us consider the case $BO_s = 1$, when $BE_{\min} = 3$, and $BE_{\max} = 5$. The first equation derives from the fact that until $j \leq W_0$, the probability of being sensed in the second backoff stage depends on the probabilities of being sensed in the first backoff stage and finding the channel busy the first or the second time. As an example, a node can arrive in $S2_1^3$ if it is in $S1_0^2$ or in $S2_0^2$, finds the channel busy, and extracts the value 0 for the second backoff stage (see Figs. 3 and 13). The second equation accounts for the fact that for $j > W_0 + 1$, there are no more transitions between the states of $BO_s = 0$ and the ones of $BO_s = 1$ because the last slot in which a node can sense the channel in the first backoff stage is $j = W_0 = 8$. Finally, when j reaches $W_1 + 3 = 19$, the sum starts with $v = 3$ and not 2, since if a node is in $S1_0^2$ (or in $S2_0^2$), it moves (in case of channel busy) to states $\{c, 1, 2, 3\}$, with $c \in [0, 15]$; therefore, the state $\{16, 1, 2, 3\}$ does not exist (see the figure).

On the other hand, if $W_{0,\ldots,k-1} > W_k$ (see Fig. 14), the probabilities of being in sensing when $CW = 2$ are given by (31), shown at the bottom of the page.

Finally, the probabilities of being in sensing when $CW = 1$, when $BO_s = k$, and with $k > 0$ are given by

$$P\left\{S1_k^j\right\} = P\left\{S2_k^{j-1}\right\} \cdot \left(1 - b_2^{j-1}\right) \tag{32}$$

for $j \in [k+3, W_{0,\ldots,k} + k]$ and null otherwise.

$$P\left\{S2_k^j\right\} = \begin{cases} \sum_{v=k+1}^{j-1} \left(P\left\{S1_{k-1}^v\right\} \cdot \frac{b_1^v}{W_k} + P\left\{S2_{k-1}^v\right\} \cdot \frac{b_2^v}{W_k}\right), & \text{for } j \in [k+2, W_k + k + 1] \\ \sum_{v=j-W_k}^{j-1} \left(P\left\{S1_{k-1}^v\right\} \cdot \frac{b_1^v}{W_k} + P\left\{S2_{k-1}^v\right\} \cdot \frac{b_2^v}{W_k}\right), & \text{for } j \in [W_k + k + 2, W_{0,\ldots,k-1} + k] \\ \sum_{v=j-W_k}^{W_{0,\ldots,k-1}+k-1} \left(P\left\{S1_{k-1}^v\right\} \cdot \frac{b_1^v}{W_k} + P\left\{S2_{k-1}^v\right\} \cdot \frac{b_2^v}{W_k}\right), & \text{for } j \in [W_{0,\ldots,k-1} + k + 1, W_{0,\ldots,k} + k - 1] \\ 0, & \text{otherwise} \end{cases} \tag{31}$$

ACKNOWLEDGMENT

The author would like to thank R. Verdone for the fruitful discussions on the model and on the paper results.

REFERENCES

[1] Part 15.4: Wireless Medium Access Control (MAC) and Physical Layer (PHY) Specifications for Low-Rate Wireless Personal Area Networks (LR-WPANs), IEEE Std. 802.15.4, 2006.

[2] Z. Aliance, *Zigbee Specifications*. San Ramon, CA: Zigbee Standard Organisation, 2008.

[3] E. Jovanov, "Wireless technology and system integration in body area networks for m-health applications," in *Proc. 27th Annu. Int. Conf. Eng. Med. Biol. Soc.*, 2005, pp. 7158–7160.

[4] R. Istepanian, E. Jovanov, and Y. Zhang, "Guest editorial introduction to the special section on m-health: Beyond seamless mobility and global wireless health-care connectivity," *IEEE Trans. Inf. Technol. Biomed.*, vol. 8, no. 4, pp. 405–414, Dec. 2004.

[5] R. Verdone, D. Dardari, G. Mazzini, and A. Conti, *Wireless Sensor and Actuator Networks*. Amsterdam, The Netherlands: Elsevier, 2008.

[6] I. F. Akyildiz, Y. S. Weilian Su, and E. Cayirci, "A survey on sensor networks," *IEEE Commun. Mag.*, vol. 40, no. 8, pp. 102–114, Aug. 2002.

[7] M. Tubaishat and S. Madria, "Sensor networks: An overview," *IEEE Potentials*, vol. 22, no. 2, pp. 20–30, Apr. 2003.

[8] G. Lu, B. Krishnamachari, and C. S. Raghavendra, "Performance evaluation of the IEEE 802.15.4 MAC for low-rate low-power wireless networks," in *Proc. Workshop EWCN*, Apr. 2004, pp. 701–706.

[9] B. Bougard, F. Catthoor, D. C. Daly, A. Chandrakasan, and W. Dehaene, "Energy efficiency of the IEEE 802.15.4 standard in dense wireless microsensor networks: Modeling and improvement perspectives," in *Proc. Des. Autom. Test Eur. Conf. Exhib.*, Mar. 2005, pp. 196–201.

[10] M. Petrova, J. Riihijarvi, P. Mahonen, and S. Labella, "Performance study of IEEE 802.15.4 using measurements and simulations," in *Proc. IEEE WCNC*, Apr. 2006, pp. 487–492.

[11] J. Misic, S. Shafi, and V. B. Misic, "Maintaining reliability through activity management in an 802.15.4 sensor cluster," *IEEE Trans. Veh. Technol.*, vol. 55, no. 3, pp. 779–788, May 2006.

[12] S. Pollin, M. Ergen, S. Ergen, B. Bougard, L. V. der Pierre, F. Catthoor, I. Moerman, A. Bahai, and P. Varaiya, "Performance analysis of slotted carrier sense IEEE 802.15.4 medium access layer," *IEEE Trans. Wireless Commun.*, vol. 7, no. 9, pp. 3359–3371, Sep. 2008.

[13] G. Bianchi, "Performance analysis of the IEEE 802.11 distributed coordination function," *IEEE J. Sel. Areas Commun.*, vol. 18, no. 3, pp. 535–547, Mar. 2000.

[14] C. Buratti and R. Verdone, "Performance analysis of IEEE 802.15.4 non-beacon enabled mode," *IEEE Trans. Veh. Technol.*, vol. 58, no. 7, pp. 3480–3494, Sep. 2009.

[15] T. Park, T. Kim, J. Choi, S. Choi, and W. Kwon, "Throughput and energy consumption analysis of IEEE 802.15.4 slotted CSMA/CA," *Electron. Lett.*, vol. 41, no. 18, pp. 1017–1019, Sep. 2005.

[16] Z. Chen, C. Lin, H. Wen, and H. Yin, "An analytical model for evaluating IEEE 802.15.4 CSMA/CA protocol in low-rate wireless application," in *Proc. IEEE AINAW*, 2007, pp. 899–904.

[17] I. Ramachandran, A. K. Das, and S. Roy, "Analysis of the contention access period of IEEE 802.15.4 MAC," *ACM Trans. Sens. Netw.*, vol. 3, no. 1, pp. 1–29, Mar. 2007.

[18] T. O. Kim, H. Kim, J. Lee, J. S. Park, and B. D. Choi, "Performance analysis of the IEEE 802.15.4 with non beacon-enabled CSMA/CA in non-saturated contition," in *Proc. Int. Conf. EUC*, Aug. 2006, pp. 884–893.

[19] J. Misic, V. B. Misic, and S. Shafi, "Performance of IEEE 802.15.4 beacon-enabled PAN with uplink transmissions in non-saturation mode—Access delay for finite buffers," in *Proc. 1st Int. Conf. BroadNets*, Oct. 2004, pp. 416–425.

[20] J. Misic, S. Shafi, and V. B. Misic, "The impact of MAC parameters on the performance of 802.15.4 PAN," *Ad Hoc Netw.*, vol. 3, no. 5, pp. 509–528, Sep. 2005.

[21] C. Buratti and R. Verdone, "A mathematical model for performance analysis of IEEE 802.15.4 non-beacon enabled mode," in *Proc. IEEE EW*, Prague, Czech Republic, Jun. 2008, pp. 1–7.

[22] L. Kleinrock, *Queueing Systems*. New York: Wiley, 1975.

[23] A. Koubaa, M. Alves, and E. Tovar, "Modeling and worst-case dimensioning of cluster-tree wireless sensor networks," in *Proc. 27th IEEE Int. RTSS*, Dec. 2006, pp. 412–421.

Chiara Buratti (M'09) was born in Ravenna, Italy, on October 30, 1976. She received the M.S. degree (*summa cum laude*) in telecommunication engineering in 2003 and the Ph.D. degree in electronics, computer science, and systems, all from the University of Bologna, Bologna, Italy.

Her research interest is on wireless sensor networks, with particular attention to routing, connectivity issues, medium-access control protocols, and the IEEE 802.15.4 standard. Since 2004, she has collaborated with such European projects as the Network of Excellence in Wireless COMmunications (NEWCOM) funded by the EC within the FP6, CRUISE, which is another Network of Excellence project funded by the EC within FP6, and NEWCOM++, which is the follow-up to NEWCOM. Since 2009, she has been involved in the Artemis project Embedded Systems for Energy Efficient Buildings (eDIANA), wherein she is the Leader of the Task devoted to the definition of topology and communication protocols.

Dr. Buratti was a corecipient of a Best Paper Award at the IEEE International Congress on Ultra Modern Telecommunications and Control Systems (ICUMT) Conference (Saint Petersburg, Russia, October 2009). She acts as a Technical Program Committee Member for several international IEEE conferences.